

***In situ* Cu doping of ultralarge CoSe nanosheets with accelerated electronic migration for superior sodium-ion storage**

Jitao Geng^a, Huilong Dong^a, Jing Liu^a, Chengkui Lv^{a,c}, Huaixin Wei^c, Yafei Cheng^{a*},
Jun Yang^{b*}, Hongbo Geng^{a*}

^aSchool of Materials Engineering, Changshu Institute of Technology, Changshu,
Jiangsu, 215500, China.

^bSchool of Material Science & Engineering, Jiangsu University of Science and
Technology, Zhenjiang, 212003, China.

^cSchool of Chemistry and Life Sciences, Suzhou University of Science and
Technology, Suzhou, 215009, China.

E-mail address: yafeicheng1990@163.com; iamjyang@just.edu.cn;
hbeng@gdut.edu.cn.

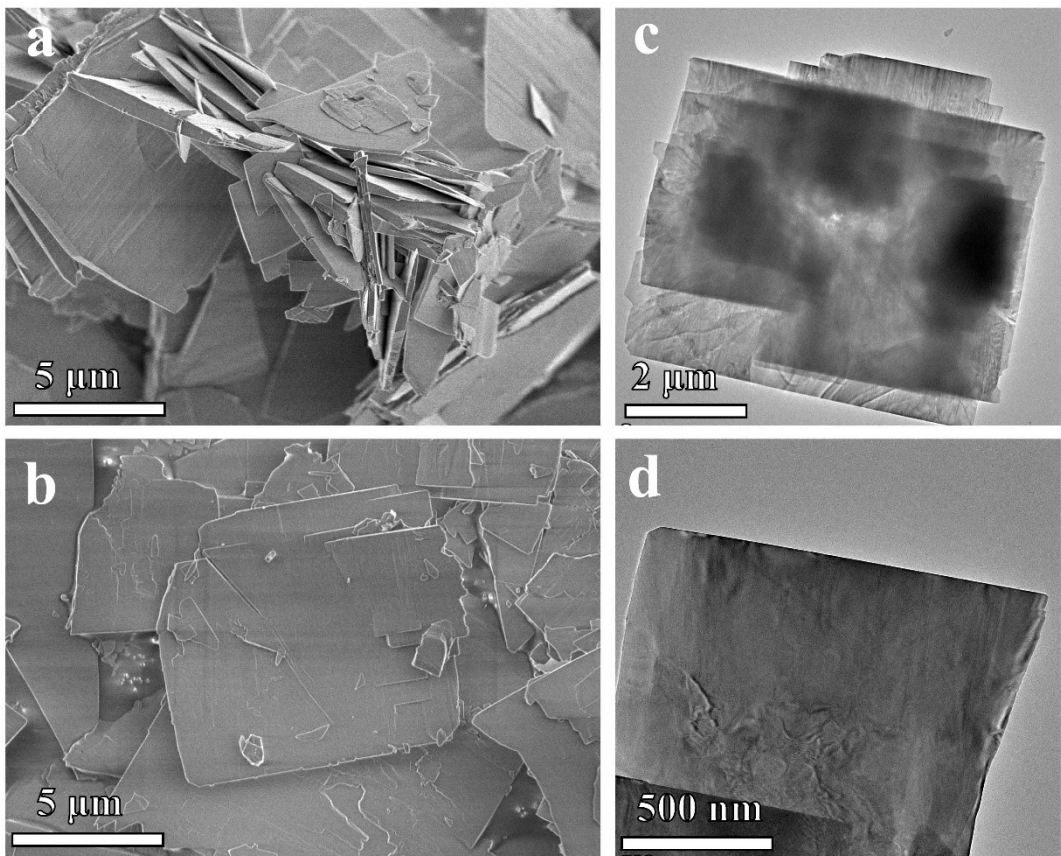


Figure S1. (a, b) SEM images and (c, d) TEM images of Cu-Co precursor.

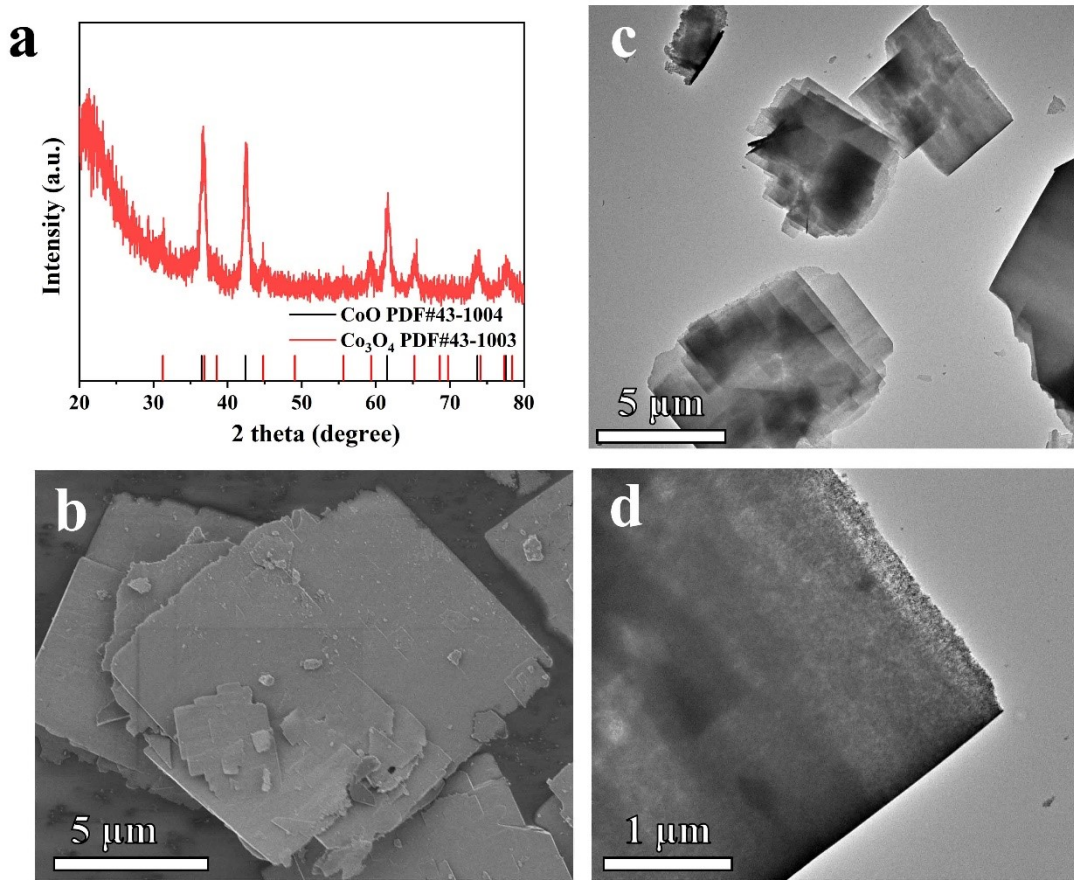


Figure S2. (a) XRD pattern, (b) SEM image and (c, d) TEM images of Cu-CoO precursor.

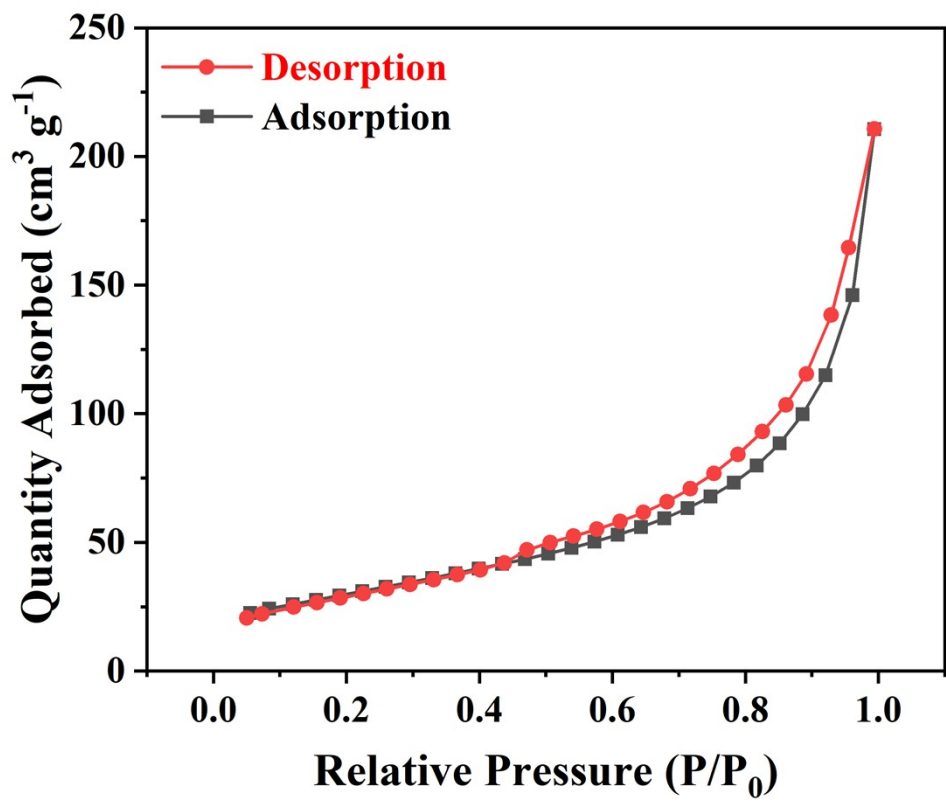


Figure S3. Nitrogen adsorption desorption curves of Cu-CoSe@NC.

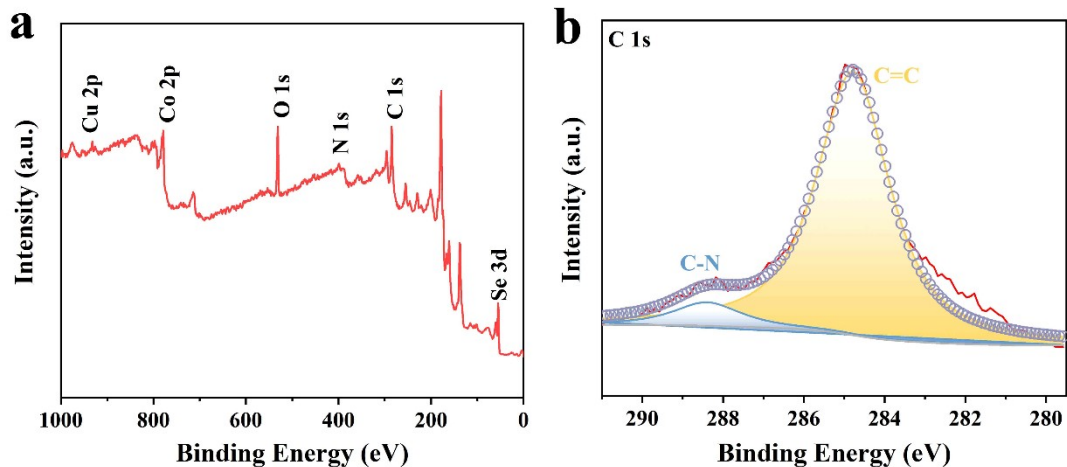


Figure S4. (a) XPS full spectrum and (b) C 1s of Cu-CoSe@NC.

Table S1. The accurate mass percentage of Co, Se, N, C, and Cu in Cu-CoSe@NC from XPS.

Element	Mass[%]	Atom[%]
C	53.00256995	81.58772134
Se	35.43540706	8.29731025
Co	23.60032031	7.403974545
O	2.310010247	2.669422109
Cu	0.142882667	0.041571756

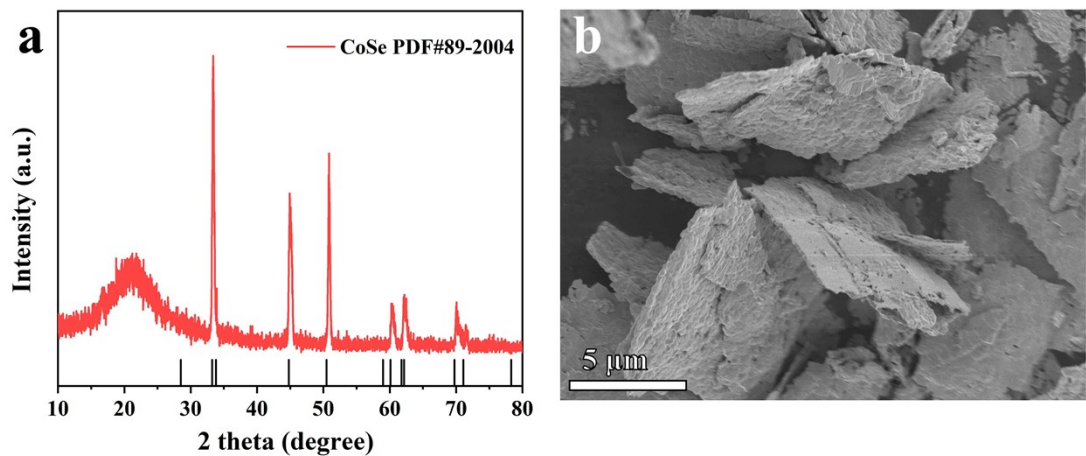


Figure S5. (a) XRD pattern, and (b) SEM image of CoSe@NC.

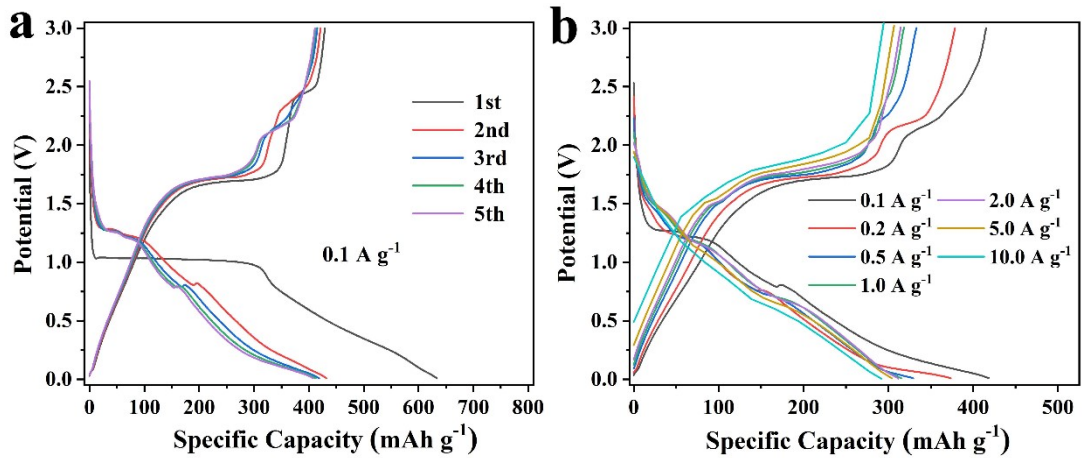


Figure S6. (a) GCD curves at 0.1 A g^{-1} , and (b) GCD curves at various current densities of CoSe@NC.

Table S2. Performance comparison of properties of selenide based anode materials

Electrode	Current density (A g^{-1})	Capacity (mAh g^{-1})	Cycling number	Reference
Cu-CoSe@NC	5	428.5	800	This work
SnSe ₂ NCs/C	1	363	1000	Ref.1
MoSe ₂ /NP-HCNS	1	210.5	1000	Ref.2
M-MoSe ₂ /NPCNF	1	212.7	1000	Ref.3
Cu–CoSe ₂	1	387	500	Ref.4
WSe ₂ /N,P-C-2	1	265	1500	Ref.5
MoSe ₂ /N-PCD	2	223	1000	Ref.6
CoSe ₂ @NC	5	354.1	800	Ref.7
S-TiSe ₂ /Fe ₃ O ₄	5	432.3	200	Ref.8
FeSe ₂ @NC-0.3	5	480	500	Ref.9
Fe-NiSe ₂ @C NS	5	302	1000	Ref.10
NM@NCNs-2	5	480	200	Ref.11
Cu doped SnSe	5	304	1000	Ref.12

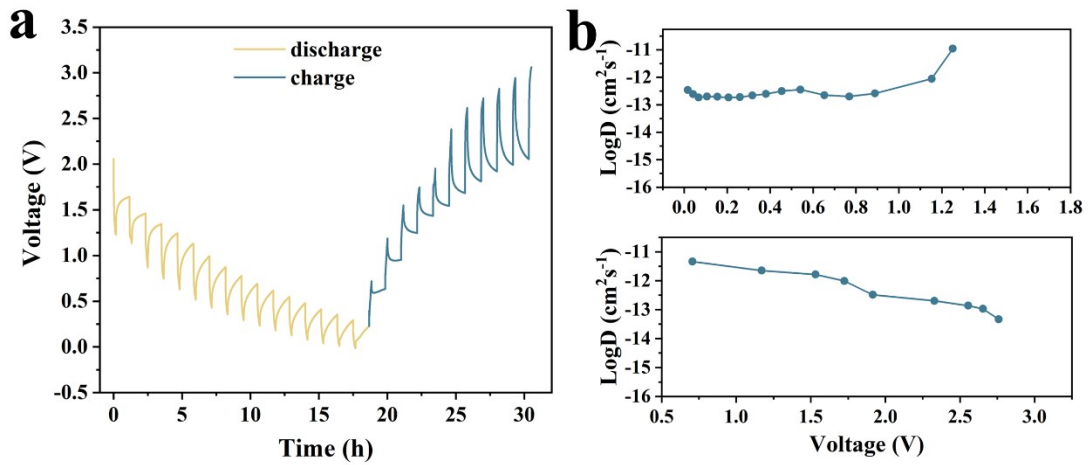


Figure S7. (a) GITT curve of pure CoSe@NC; (f) the calculated sodium-ion diffusion coefficients.

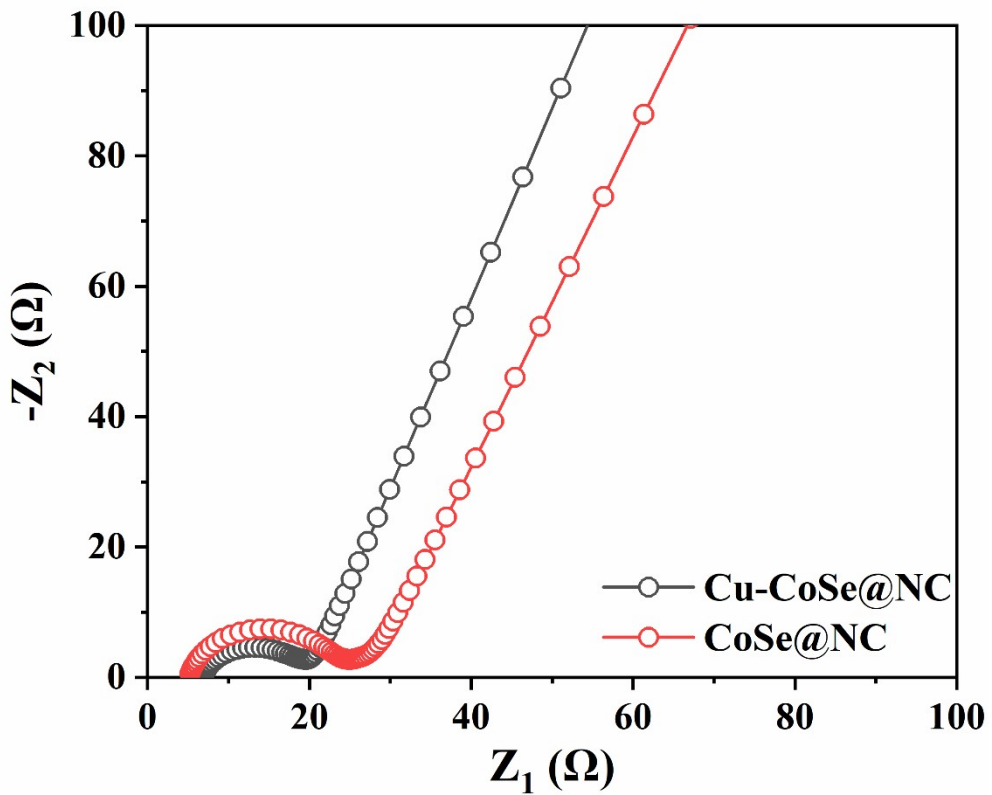


Figure S8. Nyquist plots of the Cu-CoSe@NC and CoSe@NC.

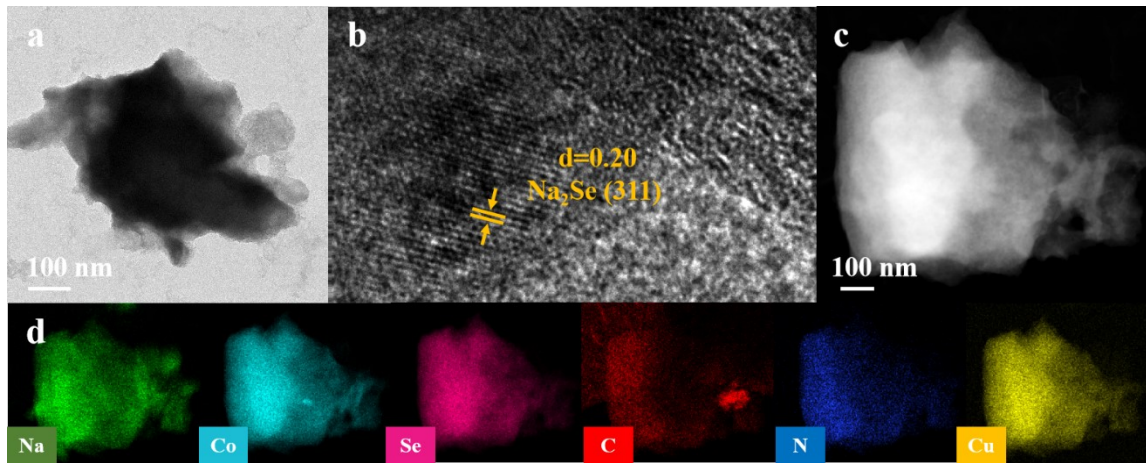


Figure S9. Ex-situ TEM patterns of the Cu-CoSe@NC anode measured at discharging to 1.0 V (0.1 A g^{-1}). (a) TEM image. (b) HRTEM image and (c, d) corresponding EDS mapping images of the electrode.

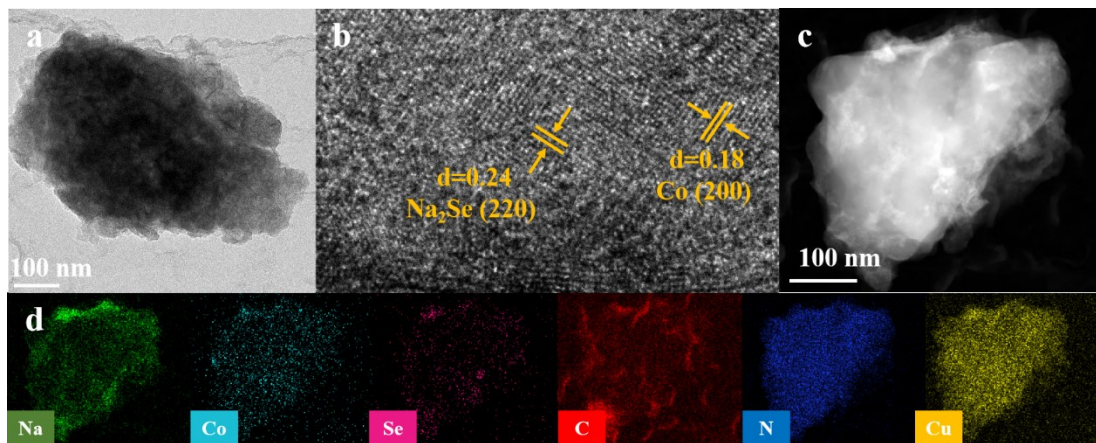


Figure S10. Ex-situ TEM patterns of the Cu-CoSe@NC anode measured at discharging to 0.01 V (0.1 A g^{-1}). (a) TEM image. (b) HRTEM image and (c, d) corresponding EDS mapping images of the electrode.

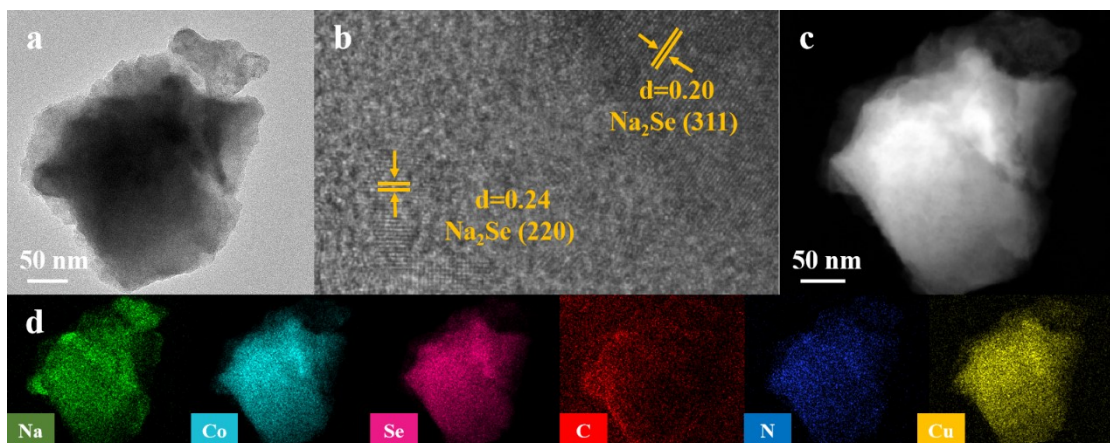


Figure S11. Ex-situ TEM patterns of the Cu-CoSe@NC anode measured at charging to 1.6 V (0.1 A g^{-1}). (a) TEM image. (b) HRTEM image and (c, d) corresponding EDS mapping images of the electrode.

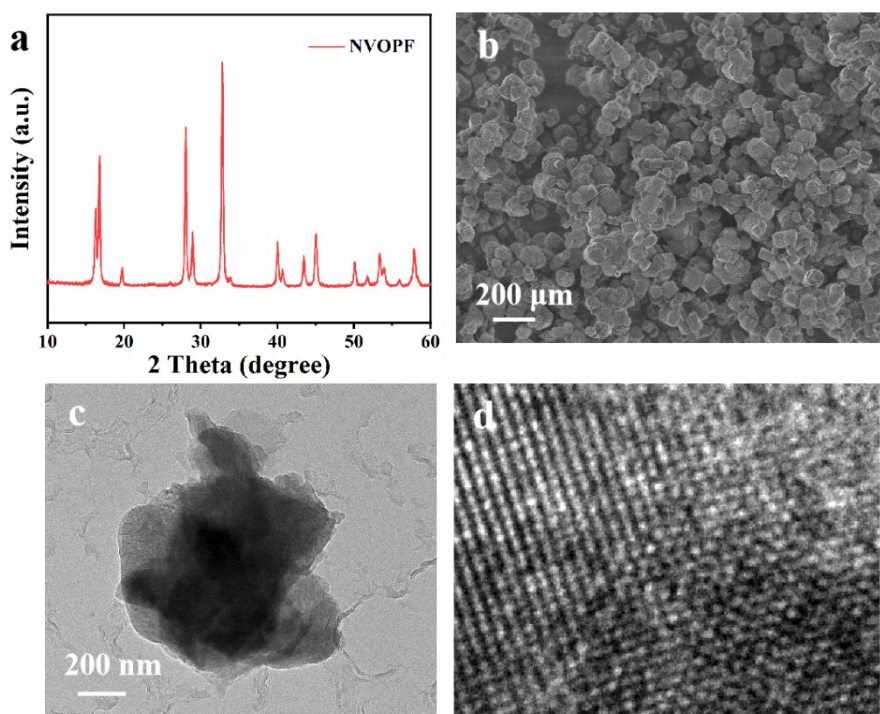


Figure S12 The XRD and morphology characterization of NVPOF.

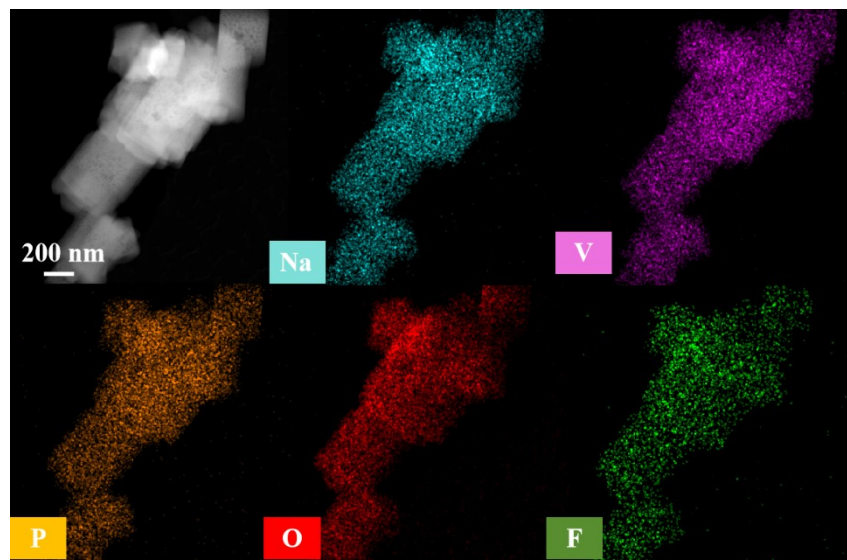


Figure S13 The corresponding EDX mapping of NVPOF.

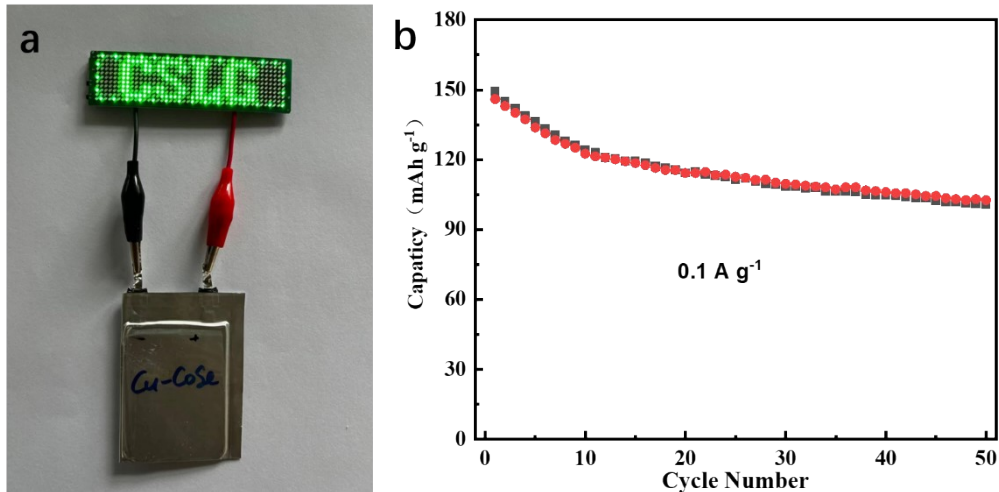


Figure S14 The image of soft package full cell and corresponding cycling performance.

References

1. H. Chen, Z. Mu, Y. Li, Z. Xia, Y. Yang, F. Lv, J. Zhou, Y. Chao, J. Wang, N. Wang, S. Guo, SnSe₂ nanocrystals coupled with hierarchical porous carbon microspheres for long-life sodium ion battery anode, *Science China Materials*, 63 (2019) 483-491.
2. L. Cui, Z. Wang, S. Kang, Y. Fang, Y. Chen, W. Gao, Z. Zhang, X. Gao, C. Song, X. Chen, Y. Wang, G. Wang, N. P Codoped Hollow Carbon Nanospheres Decorated with MoSe₂ Ultrathin Nanosheets for Efficient Potassium-Ion Storage, *ACS Appl Mater Interfaces*, 14 (2022) 12551-12561.
3. C. Li, Y. Zhang, J. Yuan, J. Hu, H. Dong, G. Li, D. Chen, Y. Li, Ultra-small few-layered MoSe₂ nanosheets encapsulated in nitrogen-doped porous carbon nanofibers to create large heterointerfaces for enhanced potassium-ion storage, *Applied Surface Science*, 601 (2022) 154196.
4. Y. Fang, X. Y. Yu and X. W. D. Lou, Formation of Hierarchical Cu-Doped CoSe₂ Microboxes via Sequential Ion Exchange for High-Performance Sodium-Ion Batteries, *Adv Mater*, 30 (2018) e1706668.
5. B. Kang, X. Chen, L. Zeng, F. Luo, X. Li, L. Xu, M.-Q. Yang, Q. Chen, M. Wei and Q. Qian, In situ fabrication of ultrathin few-layered WSe₂ anchored on N, P dual-doped carbon by bioreactor for half/full sodium/potassium-ion batteries with ultralong cycling lifespan, *Journal of Colloid and Interface Science*, 574 (2020) 217-228.
6. X. Xie, K. Huang, X. Wu, N. Wu, Y. Xu, S. Zhang and C. Zhang, Binding hierarchical MoSe₂ on MOF-derived N-doped carbon dodecahedron for fast and durable sodium-ion storage, *Carbon*, 169 (2020) 1-8.
7. J. Geng, C. Sun, J. Xie, H. Dong, Z. Wang, H. Wei, Y. Cheng, Y. Tian, H. Geng, Topological transformation construction of a CoSe₂/N-doped carbon heterojunction with a three-dimensional porous structure for high-performance sodium-ion half/full batteries, *Inorganic Chemistry Frontiers*, 9 (2022) 3176.

8. J. Yang, Y. Zhang, Y. Zhang, J. Shao, H. Geng, Y. Zhang, Y. Zheng, M. Ulaganathan, Z. Dai, B. Li, Y. Zong, X. Dong, Q. Yan and W. Huang, S-Doped TiSe₂ Nanoplates/Fe₃O₄ Nanoparticles Heterostructure, *Small*, 13 (2017) 1702181.
9. P. Wang, Y. Hou, G. Deng, Z. Liu, Y. Li, D. Zhu, D. Guo and S. Sun, FeSe₂ nanocrystalline aggregated microspheres with ultrahigh pseudocapacitive contribution for enhanced sodium-ion storage, *CrystEngComm*, 25 (2023) 3916-3921.
10. J. Liu, J. Xie, H. Dong, H. Wei, C. Sun, J. Yang and H. Geng, Iron doping of NiSe₂ nanosheets to accelerate reaction kinetics in sodium-ion half/full batteries, *Science China Materials*, 2066 (2021) 2069-2078.
11. L. Gao, H. Ren, X. Lu, S. Woo Joo, T. Xiaoteng Liu, J. Huang, Heterostructure of NiSe₂/MnSe nanoparticles distributed on cross-linked carbon nanosheets for high-performance sodium-ion battery, *Applied Surface Science*, 599 (2022) 154067.
12. R. Chen, S. Li, J. Liu, Y. Li, F. Ma, J. Liang, X. Chen, Z. Miao, J. Han, T. Wang and Q. Li, Hierarchical Cu doped SnSe nanoclusters as high-performance anode for sodium-ion batteries, *Electrochimica Acta*, 282 (2018) 973-980.